Center for Autonomous Vehicle Research (CAVR)          Faculty and Researchers' Publications

1999-07

# Testing and Evaluation of an Integrated GPS/INS System for Small AUV Navigation

Bachmann, E.R.; Healey, A.J.; Knapp, R.G.; McGhee, R.B.; Roberts, R.L.; Whalen, R.H.; Yun, X.; Zyda, M.J.

# Testing and Evaluation of an Integrated GPS/INS System for Small AUV Navigation

X. Yun, *Senior Member, IEEE*, E. R. Bachmann, R. B. McGhee, *Fellow, IEEE*, R. H. Whalen,
R. L. Roberts, R. G. Knapp, A. J. Healey, *Member, IEEE*, and M. J. Zyda, *Member, IEEE*

*Abstract*— A Small Autonomous Underwater Vehicle Nnavigation System (SANS) is being developed at the Naval Postgraduate School. The SANS is an integrated Global Positioning System/Inertial Navigation System (GPS/INS) navigation system composed of low-cost and small-size components. It is designed to demonstrate the feasibility of using a low-cost strap-down inertial measurement unit (IMU) to navigate between intermittent GPS fixes. The present hardware consists of a GPS/DGPS receiver, IMU, compass, water speed sensor, water depth sensor, and a data processing computer. The software is based on a 12-state complementary filter that combines measurement data from all sensors to derive a vehicle position/orientation estimate. This paper describes hardware and software design and testing results of the SANS. It is shown that results from tilt table testing and bench testing provide an effective means for tuning filter gains. Ground vehicle testing verifies the overall functioning of the SANS and exhibits an encouraging degree of accuracy.

*Index Terms*— AUV, complementary filter, GPS, INS, inertial navigation.

## I. INTRODUCTION

**A**UTONOMOUS underwater vehicles (AUV's) are capable of a variety of overt and clandestine missions. Such vehicles have been used for inspection, mine counter measures, survey, and observation [1]. Accurate navigation is a crucial aspect of each of these missions. The Global Positioning System (GPS) is capable of providing this accuracy if integrated with an Inertial Navigation System (INS) to compensate for intermittent reception caused by either wave action or deliberate submergence. Integrated GPS/INS systems have been applied to aircraft and space shuttle guidance and navigation [2]–[4], balloon navigation [5], missile systems [6], [7], land vehicles [8], and mobile robots [9], [10]. In these applications, GPS data are continuously available in short intervals, and INS data are used to navigate between GPS fixes. The Small AUV Navigation System (SANS) is designed to demonstrate the feasibility of using a low-cost strap-down inertial measurement unit (IMU) for AUV navigation where GPS data may not be available for an extended period of time when an AUV is submerged. The goal of the SANS is a self-contained internally or externally mountable package which can be easily carried by a small AUV. The initial

installation target for the SANS is the Naval Postgraduate School "Phoenix" AUV [11], [12].

The development of a prototype or "proof of concept" SANS was described in [13] and [14]. Experiments with the SANS and a similar system [15] support the belief that it is possible to navigate with 10-m rms accuracy for periods of up to several minutes between DGPS position fixes using a low-cost IMU. The system reported in [13] was separated into two subsystems to enable experiments using a towfish (small tow body) and was larger in size than that given as a SANS goal in [16]. The low data rate of this system appeared to be its major limitation. Replacement of the majority of the hardware components used in that prototype resulted in a compact single-unit system with a data rate ten times higher than that of the prototype [17].

Throughout the development of the SANS system, incremental improvements have been made to the 12-state constant gain complementary filter on which the software is based. The purpose of the filter is to utilize IMU, heading, and water-speed information to implement an INS and then integrate this with GPS information into a single system which produces continuously accurate navigation information in real time. Accelerometer data is used as a low-frequency data complement to high-frequency angular rate sensor data for orientation estimation and as high-frequency linear acceleration data. Proper tuning of the filter gains has proved to be a key element in system accuracy. An improved understanding of angular rate sensor bias estimation has led to the development of an effective calibration procedure for the filter [18].

Extensive tilt table and bench testing was conducted to properly tune the filter gains. Bench testing results with different gain values are presented to show the effect of the filter gains on the estimation accuracy. Ground vehicle testing was also conducted in which the SANS system was mounted on a moving golf cart. Data were collected while the cart was driven over a surveyed course. Results from ground vehicle testing demonstrate the feasibility of the current SANS system. Future work will involve at-sea testing using the Phoenix AUV.

## II. SYSTEM DESCRIPTION

### A. Hardware

The hardware configuration of the SANS has changed and improved considerably over the course of development. An earlier version of the SANS system reported in [13] was separated into two subsystems. The IMU, water-speed sensor, compass, GPS antenna, and data logging computer were configured into one package and placed in a towfish. The
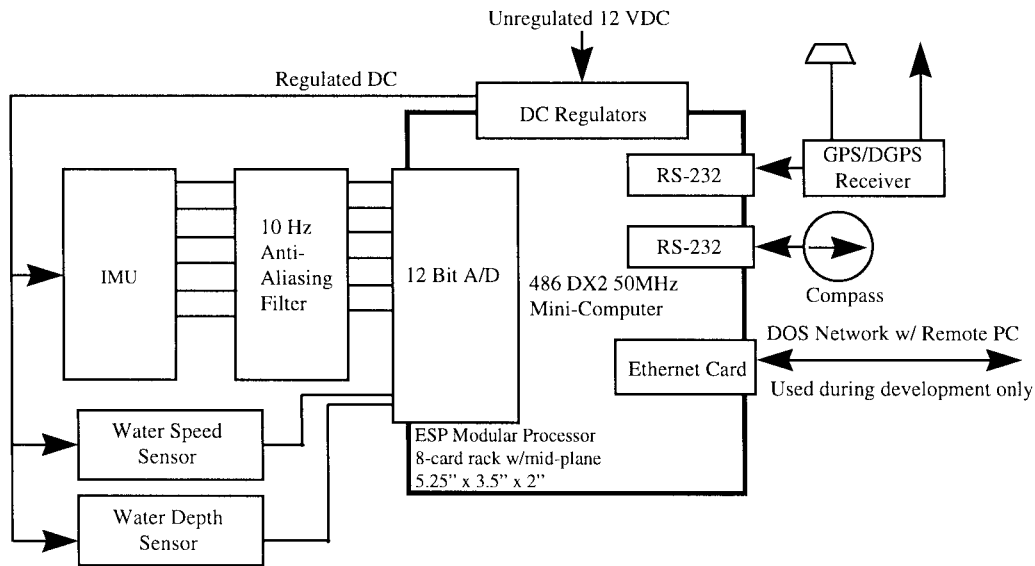
Fig. 1.   Block diagram of the new SANS hardware configuration.

GPS receiver, DGPS antenna, and data processing computer were placed in a towing vessel. The data collected by the towfish subsystem were transmitted to the data processing computer through a modem connection. It was found in these experiments that wave splash on the GPS antenna had no serious effect on GPS signal reception during time periods when the towfish was surfaced [13].

The current hardware configuration of the SANS system is shown in Fig. 1. All the components in this configuration are physically packaged in a single self-contained box with dimensions $6 \times 17 \times 3$ in [17]. Supplying it with a 12-V dc power source (e.g., a 12-V dc battery) is all that is needed to make the system operational. The on-board processor is an Extremely Small Package (ESP) Cyrix 486SLC DX2 50 MHz computer running the DOS operating system. With this processor alone, a sampling rate of about 4 Hz was achieved [17]. In the current configuration, a floating point math coprocessor was integrated, resulting in a tenfold increase in sampling rate from 4 to 40 Hz [18]. The current SANS system is also equipped with an Ethernet card that allows it to be connected to another computer(s) via a TCP/IP network during development phase. This Ethernet interface has proved to be an extremely useful tool for transferring programs, logging data, monitoring the system status, etc.

To improve the performance and reliability of the SANS system, the ESP on-board processor is to be replaced by an AMD 586DX133 based PC/104 module computer.

### B. Software

The current SANS navigation software is based on a 12-state complementary filter shown in Fig. 2. The 12 state variables are the outputs of each of the three integrator blocks, estimated current in north and east directions, and the bias estimates for the angular rate readings. The state variables are shown in Table I. In Fig. 2, $R(\phi, \theta, \psi)$ is a rotation matrix [19] and $T(\phi, \theta, \psi)$ is a body-rate-to-Euler-rate transformation matrix [20].

TABLE I
STATE VARIABLES OF THE COMPLEMENTARY FILTER

| | |
|---|---|
| Euler Angles | $\phi, \theta, \psi$ |
| North & East Velocity | $\dot{x}_e, \dot{y}_e$ |
| North & East Position | $x_e, y_e$ |
| Apparent Current | $\dot{x}_c, \dot{y}_c$ |
| Angular Rate Bias Estimates | $p_b, q_b, r_b$ |

In the filter depicted in Fig. 2, all gains are constant and are initially determined by bandwidth considerations, followed by experimental tuning. Since all gain matrices have thus far been constrained to be diagonal, the approach taken to date is based on the concept of "complementary filtering" [21], [13], [14]. The results presented in this paper indicate that this approach works well.

### III. SYSTEM COMPONENTS TESTING

Filter gains $K_1, K_2, K_3$, and $K_4$ are initially assigned based on bandwidth considerations and subsequently tuned based on component experimental testing. Tilt table testing was conducted to tune $K_1$. Bench testing was carried out to adjust $K_3$ and $K_4$. A calibration of the magnetic compass resulted in better tuning of $K_2$. Each of these experiments is described below in more detail.

### A. Tilt Table Testing Results

Due to the aperiodic nature of the SANS filter and a lack of statistical data on errors in the data sensed by the towfish, analytic determination of satisfactory values for the gain matrices and proper scale factors for the input data has proved difficult [22]. Consequently, in order to be able to precisely control input to the filter, the SANS unit was placed on a Haas rotary tilt table, Model TRT-7 [23]. The table has two degrees of freedom (DOF) and is capable of positioning to an accuracy of 0.001 degrees at rates ranging from 0.001 to 80 degrees/s.

Accelerometers $(\ddot{x}_a, \ddot{y}_a, \ddot{z}_a)$

$\theta_a = \mathrm{asin}\dfrac{\ddot{x}_a}{g}$

$\phi_a = -\mathrm{asin}\dfrac{\ddot{y}_a}{g \cdot \cos\theta}$

Estimated Bias $(p_b, q_b, r_b)$

$\phi_a, \theta_a$

$K_1$

Angular-rate Sensors $(p, q, r)$

$T(\phi, \theta, \psi)$

$\dot{\phi}_s, \dot{\theta}_s$

$\dot{\psi}_s$

$\int$

$\phi, \theta$

Euler Angles $\psi$

$K_2$

Euler Angles $(\phi, \theta, \psi)$

Magnetic Compass $(\psi_c)$

Local Magnetic declination

Accelerometers $(\ddot{x}_a, \ddot{y}_a, \ddot{z}_a)$

$\ddot{x} = \ddot{x}_a - g\sin\theta$
$\ddot{y} = \ddot{y}_a + g\sin\phi \cdot \cos\theta$
$\ddot{z} = \ddot{z}_a + g\cos\phi \cdot \cos\theta$

$(\ddot{x}, \ddot{y}, \ddot{z})$

$R(\phi, \theta, \psi)$

North & East Accel $(\ddot{x}_e, \ddot{y}_e)$

North & East Velocity $(\dot{x}_e, \dot{y}_e)$

North & East Position $(x_e, y_e)$

$\int$

$(\dot{x}_w, \dot{y}_w)$

$K_3$

Apparent Current $(\dot{x}_c, \dot{y}_c)$

Weighted Reset

GPS Position

Water Speed $u_w$

$R(\phi, \theta, \psi)$

Euler Angles $(\phi, \theta, \psi)$

$\Sigma$

$K_4$

$\dfrac{1}{\Delta t}$

Interval Between GPS Fixes
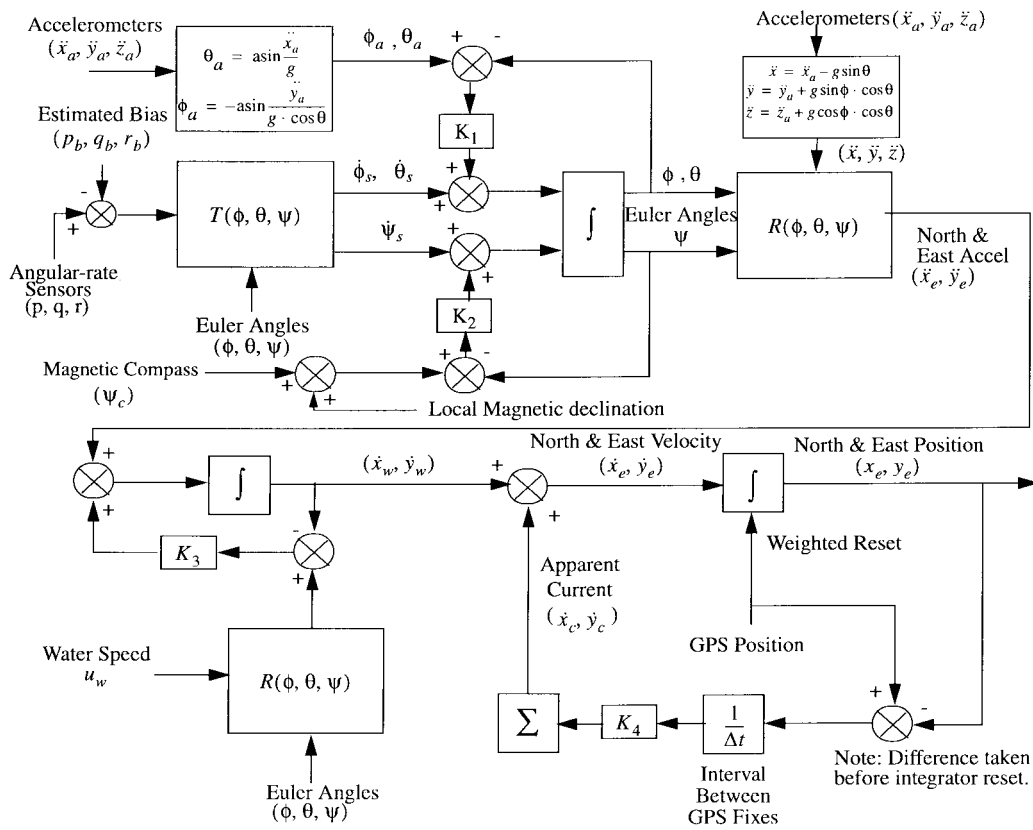
Note: Difference taken before integrator reset.

Fig. 2. Diagram of the SANS navigation filter.

Tuning data for the SANS was obtained by moving the SANS unit through each DOF at varying rates within a 45° range. The attitude as determined by the SANS was then plotted and compared with the actual motion of the unit. Through this comparison, it was possible to determine initial gain values and scale factors. The tilt table data was then postprocessed using these initial values and once again compared to the actual motion of the SANS unit. This process was repeated several times until the attitude determined by the filter "matched" the true motion of the unit. Angular rate biases are estimated by a low-pass filter with a time constant of 1000 s.

Fig. 3 shows an example of the results obtained during the tuning process. The slight overshoots following each motion may indicate that the scale factor for the $y$ axis angular rate sensor is slightly high. However, this effect may also be due to undersampling problems. The flatness of the curve following stabilization after each motion indicates that a reasonable gain value has been determined as does the distance between the tails of each step.

As exemplified by Fig. 3, tilt table tests of the SANS system show that attitude sensing is achieved to an accuracy of one degree or better under the most demanding of circumstances [18]. This is in agreement with the findings of other investigations [24].

### B. Bench Testing Results

To tune filter gains $K_3$ and $K_4$, a series of bench tests were conducted. The SANS system was mounted on a golf cart.[1]

[1] See Section IV on ground vehicle testing for the purpose of using a golf cart.

The cart was parked throughout bench testing. The DGPS receiver was programmed to provide a GPS fix every 2 s. Since water speed is obviously unavailable in bench testing, an artificial constant water speed was entered in the filter program in place of water speed data. In what follows, results for constant speed inputs of 0.0 and 10.0 ft/s will be presented.

Figs. 4 and 5 depict the testing results with water speed being set to zero. In this test, the filter gains were chosen to be: $K_1 = 0.1$, $K_2 = 0.5$, $K_3 = 2.0$, and $K_4 = 0.01$. Fig. 4 shows the estimated position in the northeast coordinates. Since the test is conducted on a stationary bench, the position trajectories should stay at the origin in an ideal case. The SANS estimate of position is within an area of $10 \times 10$ ft$^2$. The drift in the position estimate is due mainly to GPS errors. The estimated currents in the north and east directions are shown in Fig. 5. Ideally they should be zero. The small amount of estimated currents is due to the drift in the position estimate caused by GPS errors.

In the next series of tests, water speed is set to 10.0 ft/s in the filter program. $K_4$ is varied from 0.01 to 1.0 while keeping all other gain values constant. Since the SANS system remains stationary on a heading of true north, a current estimate of $-10.0$ ft/s is expected if the SANS filter works correctly. Fig. 6 shows the current estimate for $K_4 = 0.1$. Just as expected, the estimated current in the north direction converges to $-10.0$ and that in the east direction is about zero. A smaller $K_4$ makes the filter slower and less responsive for the estimation of the current. For example, for $K_4 = 0.01$, the filter takes about 400 s to reach the steady-state estimated value. A larger $K_4$ makes the filter more responsive but results in a noisier estimate.
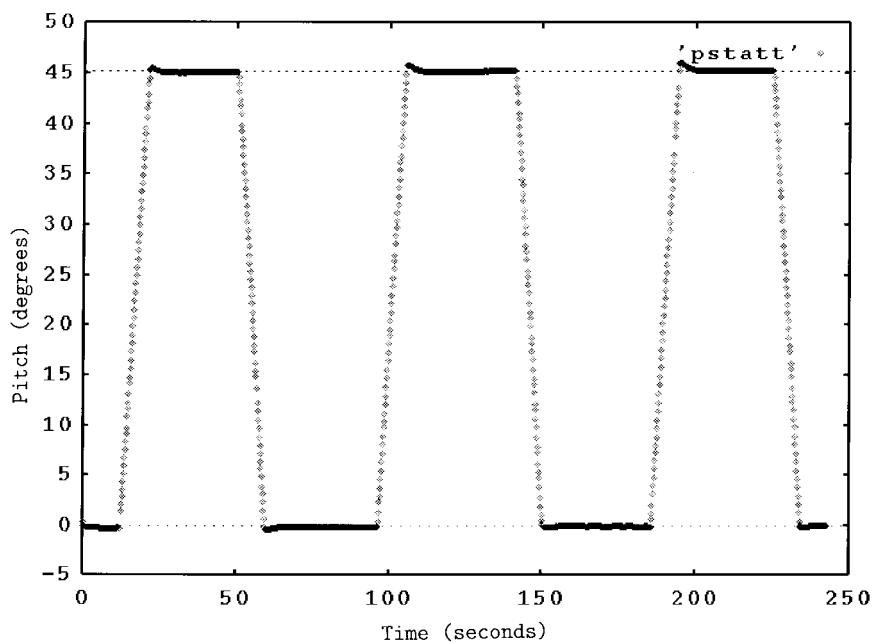
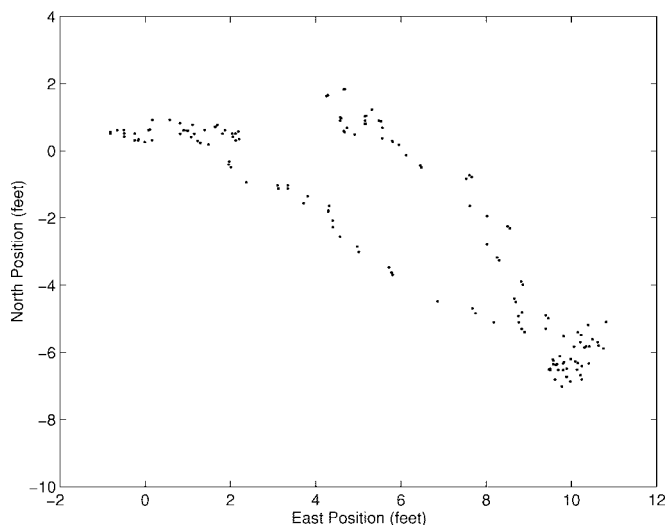Fig. 3. Forty-five degree pitch excursions at 5 degrees/s.



Fig. 4. Position plot of bench testing with water speed being set to zero, $K_1 = 0.1$, $K_2 = 0.5$, $K_3 = 2.0$, and $K_4 = 0.01$ for a duration of 160 s.
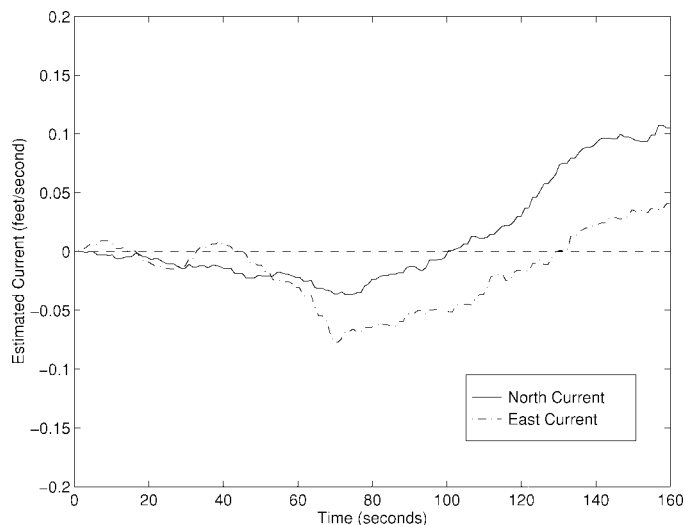


Fig. 5. Estimated current for bench testing with water speed being set to zero, $K_1 = 0.1$, $K_2 = 0.5$, $K_3 = 2.0$, and $K_4 = 0.01$.

Similar testing was conducted for tuning $K_3$. The estimated current of one typical experiment is presented in Fig. 7. In this particular case, $K_3$ is reduced from 2.0 (the value that was used in all the previous tests) to 0.5. $K_4$ is set to 0.5 as well. Comparing Fig. 7 with Fig. 6, it is evident that larger $K_3$ values produce a better performance. This is not surprising since a larger $K_3$ places more confidence on water speed that is constant and free of noise during bench testing. The proper value for $K_3$ must be determined again with real water speed data when at-sea testing is performed.

## C. Compass Calibration Results

To obtain the heading information in the SANS, the angular rate sensor is used as a high-frequency input source and the digital compass (Precision Navigation Electronic Compass,

Model TCM2) is used as a low-frequency data source. In a series of ground vehicle tests (see Section IV for more details), it was noted that the SANS heading was off by a few degrees. Fig. 8 shows a typical run of ground vehicle testing with a GPS update every 10 s. The solid line is the filtered vehicle track with continuous GPS data and is taken as a reference. The dotted line is the filtered vehicle track when GPS information is provided to the filter every 10 s. The vehicle starts from the $(0,0)$ coordinate, moves westward, continues northward after a right turn, and returns to the starting location after making a U-turn. It is evident, particularly from the northerly run, that the filter is not receiving accurate directional information. A comparison of raw compass data and the filtered heading points to the compass as the source of heading error.
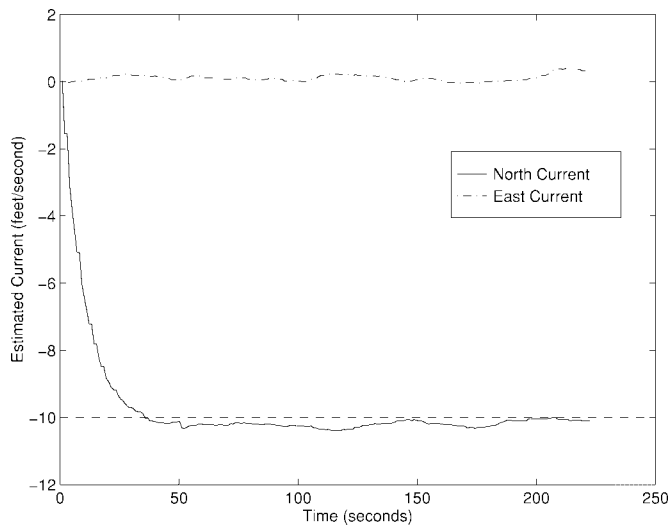
Fig. 6.   Estimated current for bench testing with water speed being set to 10.0 ft/s, $K_1 = 0.1$, $K_2 = 0.5$, $K_3 = 2.0$, and $K_4 = 0.1$.
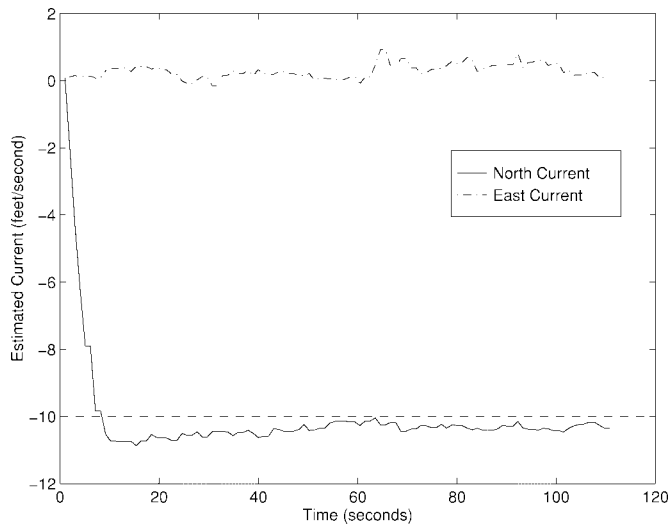


Fig. 8.   Position plot prior to compass calibration from ground vehicle testing with a GPS update every 10 s.



Fig. 7.   Estimated current for bench testing with water speed being set to 10.0 ft/s, $K_1 = 0.1$, $K_2 = 0.5$, $K_3 = 0.5$, and $K_4 = 0.5$.
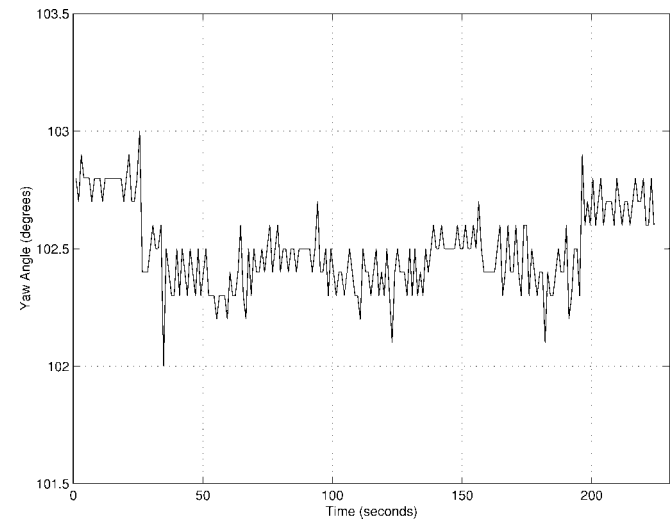


Fig. 9.   Effect of the golf cart motor on compass measurements.

The investigation of compass deviation was focused on three areas: possible interference produced by the golf cart electric motor, vibration, and the deviation of the compass itself. The TCM-2 compass has a self calibration routine which is supposed to remove the effects of static magnetic fields caused by ferrous materials in the vicinity of the compass. The calibration routine is not capable of compensating for dynamic magnetic field distortions like those caused by an electric motor. To find the qualitative effect of the electric motor on the compass, a series of tests were performed.

The tests were performed by jacking up the rear wheels of the golf cart so that they could spin freely while the motor was on. The motors were turned on for 30-s intervals followed by a 30-s off time. During the off time, the wheels continued to rotate for approximately 10–15 s until they came to a stop. This test allowed changes in heading due to motor engagement to be observed. The same test was performed four times rotating the cart through the cardinal points. The result of one such test
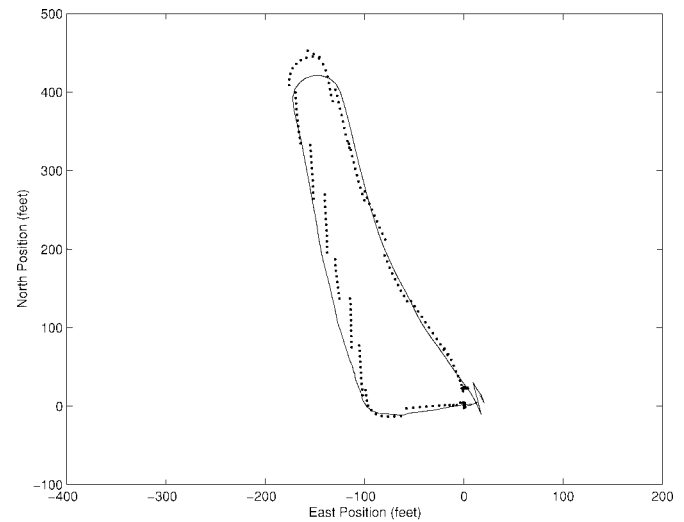
(with the vehicle facing east) is depicted in Fig. 9. Testing results indicate that there is interference, but its magnitude appears to be limited to approximately a half of a degree. The figure also indicates that the noise is at a relatively high frequency which can be compensated for with an appropriate value for $K_2$. Similar results were obtained with a full load applied to the motor.

The effect of vibration was tested by lightly tapping the compass board with a screwdriver and a finger. Fig. 10 shows a compass reading obtained in this experiment. It is seen that vibration clearly plays a much greater role in compass error than the electric motor. However, these deviations are mostly in a high-frequency range and can be filtered out with an appropriate choice of $K_2$.

In ground vehicle testing, it was noticed that the heading error during east–west runs was not as large as during north–south runs. A final test was conducted to determine if compass deviations that are heading-dependent are present. The test was performed by swinging the compass and com-
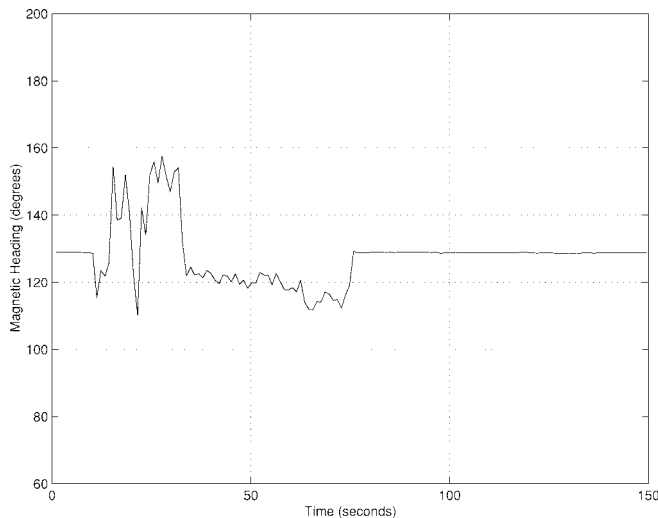
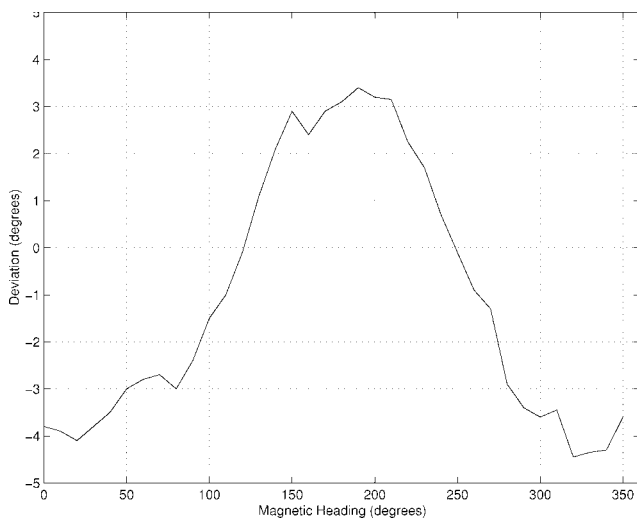Fig. 10.   Effect of vibration on compass measurements.



Fig. 12.   The towfish mounted on a golf cart during parking lot testing.



Fig. 11.   TCM-2 compass deviation.
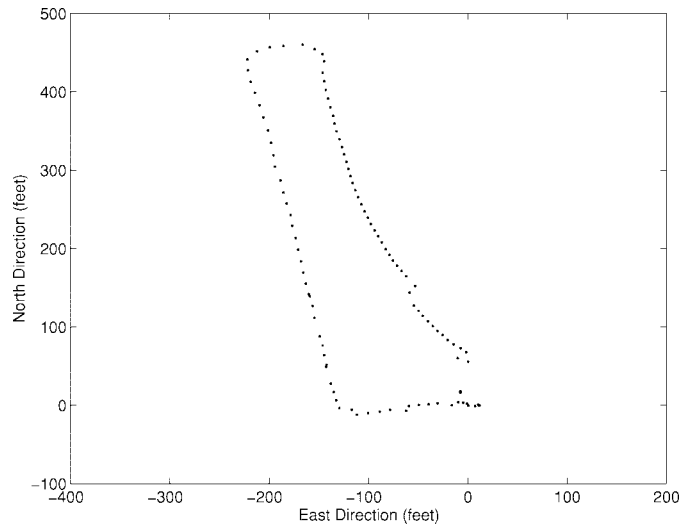


Fig. 13.   Position plot in 1-s increments from golf cart testing in the parking lot.

paring the compass reading with a reference. The instrument used as the reference was a transit manufactured by W. and L. E. Gurley with an accuracy of 0.5 degrees. It has a calibrated balanced magnetic compass mounted within its body. By mounting the transit in line with the TCM-2 compass, a comparison is made between the two indicated headings. The compass was swung through the entire 360°, taking measurements every 10°. Fig. 11 shows the difference between measurements of the transit and those of the TCM-2 compass. Fig. 11 is qualitatively in agreement with the observation made during ground vehicle testing where north–south runs show greater heading errors than east–west runs. Using this data, a lookup table and linear interpolating function was added to the SANS filter code to compensate for the heading-dependent deviation. It is noted that both TCM-2 compass and transit measure magnetic heading, while DGPS provides the geographic North. As shown in Fig. 2, the magnetic declination of 15° in Monterey, CA, is compensated for in software.

To eliminate high-frequency effects of dc motors and vibration, the value of $K_2$ was decreased from its previous value

of 0.5–0.1. This corresponds to a time constant of 10 s, which makes the filter less responsive to high-frequency transients caused by dc motors and vibration.

## IV.   GROUND VEHICLE TESTING

In addition to tilt table testing and bench testing, a series of ground vehicle tests were performed in preparation for at-sea testing. In ground vehicle testing, the SANS system was installed on a golf cart, as shown in Fig. 12. The cart was driven around a surveyed course in a moderately sloped parking lot. Due to a lack of speed measurements in the initial tests, the cart was driven in the parking lot for a number of complete turns with constant accelerator foot pedal position, and the total traveling time was measured. An average speed was calculated based on the observed time and length of the course and hand coded into the software.

Results from one representative ground vehicle test are presented in Figs. 13–17. During this test, the filter gains were set to: $K_1 = 0.1, K_2 = 0.5$, $K_3 = 2.0$, and $K_4 = 0.01$.
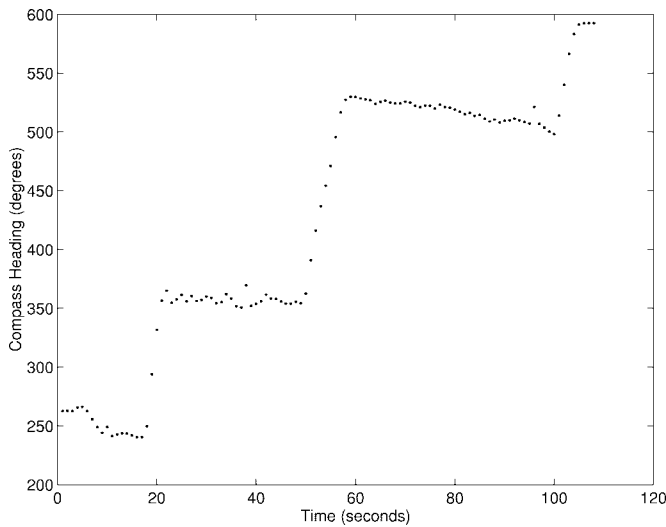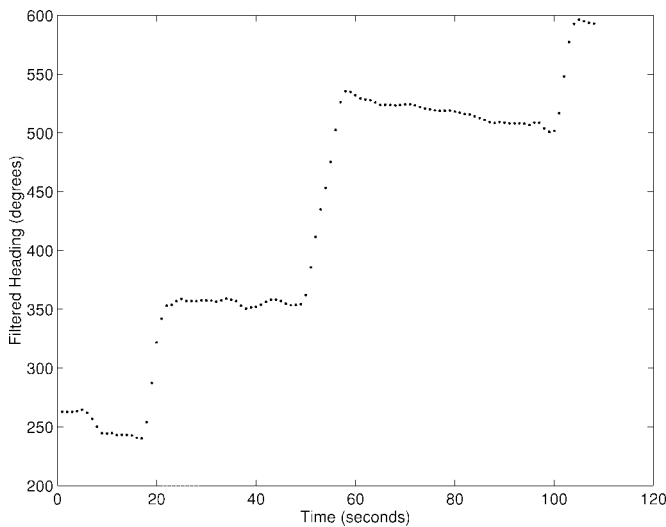
Fig. 14.   Compass heading from ground vehicle testing.



Fig. 16.   Estimated east current (ft/s).



Fig. 15.   Filtered heading from ground vehicle testing.



Fig. 17.   Estimated north current (ft/s).

The calculated average cart speed is 11.6 ft/s. Continuous DGPS data was available throughout this test. Fig. 13 shows the estimated position trajectory of the cart. The cart started from the $(0,0)$ position and traveled westward for about 120 ft before making the first right turn. The cart then traveled northward for about 450 ft, made a U-turn, and returned to the starting point along the other leg of the parking lot driveway. The parking lot is flat with a slight downward slope toward the north end. All data were collected at 1-s intervals. The effect of this slope on cart speed can be observed by comparing the fix spacing on the northbound and southbound legs.

Fig. 14 shows the heading from raw compass data, while Fig. 15 shows the heading produced by the navigation filter. Similarity is clearly observed in these two plots. It can be seen that, as expected, the filter output is smoother than the raw compass data. The heading is in agreement with the position plot.

The estimated current is plotted in Figs. 16 and 17. As mentioned earlier, the average speed of the cart was computed and input into the program in place of speed through the water.
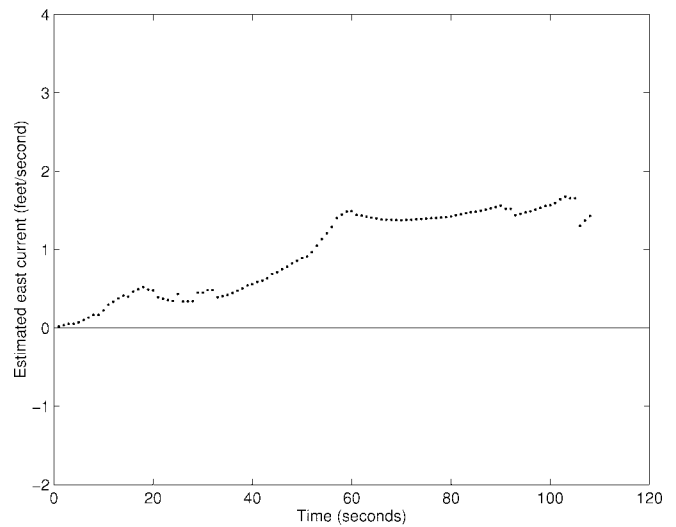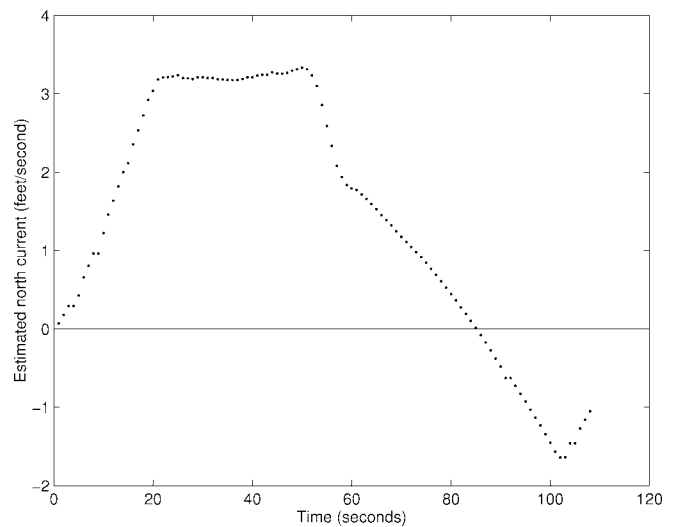
If the cart moves faster than the assumed average speed, the filter will attribute the difference to current. Since the parking lot has a downward slope from the south (starting) end to the north end, the cart moves faster northward (out bound leg), and slower southward (return leg). This is evident from the denseness of dots in Fig. 13 since data were collected at equal time intervals. The dots along the left leg of the plot are visibly sparser than those along the right leg. From the heading plots, it is seen that the cart started making the U-turn at about 50 s. Prior to the U-turn, the filter estimated a positive north current of 3.2 ft/s, as shown in Fig. 17. From the first right turn until the U-turn, the cart traveled some 450 ft in about 30 s (from 20 to 50 s in time). The actual average speed along this segment of path is thus 15.0 ft/s, which is 3.4 ft/s faster than the speed (11.6 ft/s) programmed into the filter. Therefore, the filter successfully estimated the current. After the U-turn, the filter qualitatively predicted the slowdown of the cart speed, but was not able to converge prior to the end of the test. This is because $K_4$ was set to 0.01 in this test. The corresponding time constant is 100 s. It will thus take about 400 s for the
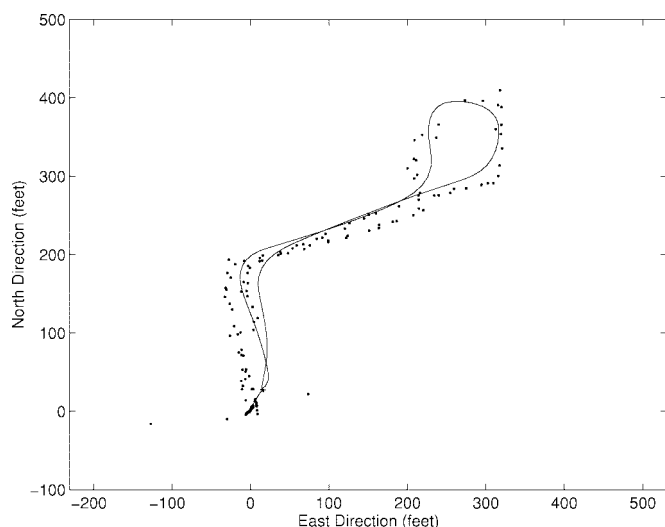
Fig. 18. Ground vehicle test result with a calibrated compass and bicycle wheel speed measurement. Dotted line: with GPS; solid line: without GPS.

filter to converge. That is, the experiment duration was too short for the filter to converge. More ground vehicle testing is planned with a larger $K_4$ (thus smaller time constant) and longer testing duration.

The ground vehicle tests described above were conducted with continuous DGPS data. The vehicle speed was crudely estimated based on the length of the traveling course and traveling time and assumed a constant value throughout testing. To better estimate the vehicle speed, a bicycle wheel was instrumented and trailed behind the golf cart. The bicycle wheel was provided with a reed switch and a magnet that generates a pulse upon every revolution. Counting the elapsed time between two pulses provides a better estimate of the average speed [25].

After implementing the bicycle wheel speed measurement and compensating for heading-dependent compass deviation (based on Fig. 11), another ground vehicle test was conducted over a different course. The result of this test is depicted in Fig. 18. The dotted line represents the vehicle trajectory with continuous GPS data. The solid line is the trajectory of the vehicle following the same path without GPS data during the entire run of 3.2 min. Taking the dotted line as the reference, it is seen that the result of dead reckoning navigation without GPS is accurate to within 10 m or better throughout this period of operation. This is encouraging and it is hoped that this accuracy can also be demonstrated in submerged navigation during at-sea testing.

## V. CURRENT AND FUTURE WORK

This technical communication presents the current status of the continuing SANS research and development effort. More hardware/software upgrades and experiments are in progress. In particular, the onboard ESP computer is being replaced by an industrial standard PC/104 computer. The paddle-wheel water speed sensor used in earlier experiments [13] will be replaced by a more accurate ultrasonic water velocity sensor. An eight-state asynchronous Kalman filter is being implemented for position and current estimation to replace the

*ad hoc* implementation of this function shown in Fig. 2 [26]. At-sea testing will be conducted when hardware and software upgrades are completed.

## VI. CONCLUSIONS

This technical communication reports on research progress in the development of the SANS system. The new hardware configuration of the system allows all the components to be packaged in a single self-contained box. The sampling rate of the system is ten times faster than the previous prototype. Laboratory testing and ground vehicle testing on a golf cart were conducted to validate proper working of the new configuration, to tune filter gains, and to confirm the feasibility of the SANS concept. Test results indicate that filter gains, for the most part, can be tuned relying on convenient bench testing together with tilt-table and ground vehicle testing. Evaluation of GPS multipath effects and other wave-induced errors awaits future at-sea testing.

## REFERENCES

[1] J. Yuh, *Underwater Robotic Vehicles: Design and Control.* Albuquerque, NM: TSI Press, 1995.
[2] R. A. Gray and P. S. Maybeck, "An integrated GPS/INS/BARO and radar altimeter system for aircraft precision approach landings," in *Proc. IEEE 1995 National Aerospace and Electronics Conf.*, Dayton, OH, May 1995, pp. 161–168.
[3] K. Braden, C. Browing, H. Gelderloos, and F. Smith, "Integrated inertial navigation system/global positioning system INS/GPS for manned return vehicle autoland application," in *Proc. IEEE 1990 Position Location and Navigation Symp.*, Mar. 1990, pp. 74–82.
[4] G. Barnes, "INS/GPS space application for all flight dynamics—Boost through landing," in *Proc. IEEE 1996 Position Location and Navigation Symp.*, Apr. 1996, pp. 457–463.
[5] C. Jekeli, "Balloon gravimetry using GPS and INS," *IEEE Aerosp. Electron. Syst. Mag.*, vol. 7, no. 6, pp. 9–15, June 1992.
[6] R. S. Ornedo and K. A. Farnsworth, "GPS and radar aided inertial nagivation system for missile system applications," in *Proc. IEEE 1998 Position Location and Navigation Symp.*, Palm Springs, CA, Apr. 1998, pp. 614–621.
[7] M. K. Martin, "New low cost avionics with INS/GPS for a variety of vehicles," in *Proc. AIAA/IEEE Digital Avionics Systems Conf.*, Oct. 1997, pp. 8.3-1–8.3-8.
[8] R. Tranfield, "INS/GPS navigation systems for land applications," in *Proc. IEEE 1996 Position Location and Navigation Symp.*, Apr. 1996, pp. 391–398.
[9] B. Barshan and H. F. Durrant-Whyte, "Inertial navigation systems for mobile robots," *IEEE Trans. Rob. Automat.*, vol. 11, pp. 328–342, June 1995.
[10] S. Sukkarieh, E. M. Nebot, and H. F. Durrant-Whyte, "Achieving integrity in an INS/GPS navigation loop for autonomous land vehicle applications," in *Proc. 1998 IEEE Int. Conf. Robotics and Automation*, Leuven, Belgium, May 1998, pp. 3437–3442.
[11] D. B. Marco, A. J. Healey, and R. B. McGhee, "Autonomous underwater vehicle: Hybrid control of mission and motion," *Autonomous Robots*, vol. 3, nos. 2/3, pp. 169–186, June 1996.
[12] D. Brutzman, T. Healey, D. Marco, and B. McGhee, "The Phoenix autonomous underwater vehicle," in D. Kortenkamp, R. P. Bonasso, and R. Murphy, Eds., *Artificial Intelligence and Mobile Robots: Case Studies of Successful Robot Systems.* Cambridge, MA: MIT Press, 1998, ch. 13, pp. 323–360.
[13] R. B. McGhee, J. R. Clynch, A. J. Healey, S. H. Kwak, D. P. Brutzman, X. P. Yun, N. A. Norton, R. H. Whalen, E. R. Bachmann, D. L. Gay, and W. R. Schubert, "An experimental study of an integrated GPS/INS system for shallow-water AUV navigation (SANS)," in *Proc. 9th Int. Symp. Unmanned Untethered Submersible Technology (UUST)*, Durham, NH, Sept. 1995.
[14] E. R. Bachmann, R. B. McGhee, R. H. Whalen, R. Steven, R. G. Walker, J. R. Clynch, A. J. Healey, and X. P. Yun, "Evaluation of an integrated GPS/INS system for shallow water AUV navigation," in *1996 IEEE*

*Symp. Autonomous Underwater Vehicle Technology*, Monterey, CA, June 1996, pp. 268–275.

[15] R. L. Thorne, "Asynchronous data fusion for AUV navigation using extended Kalman filtering," Master's thesis, Naval Postgraduate School, Monterey, CA, Mar. 1997.

[16] S. H. Kwak, J. B. McKeon, J. R. Clynch, and R. B. McGhee, "An experimental investigation of GPS/INS integration for small AUV navigation," in *Proc. 8th Int. Symp. Unmanned Untethered Submersible Technology (UUST)*, Durham, NH, Sept. 1993.

[17] R. G. Walker, "Design and evaluation of an integrated, self-contained GPS/INS shallow-water AUV navigation system (SANS)," Master's thesis, Naval Postgraduate School, Monterey, CA, June 1996.

[18] R. L. Roberts, "Implementation and evaluation of an integrated self-contained GPS/INS shallow-water AUV navigation system (SANS)," Master's thesis, Naval Postgraduate School, Monterey, CA, Mar. 1997.

[19] J. J. Craig, *Introduction to Robotics: Mechanics and Control*, 2nd ed. Reading, MA: Addison-Wesley, 1989.

[20] R. B. McGhee and A. A. Frank, "Some considerations relating to the design of autopilots for legged vehicles," *J. Terramechan.*, vol. 6, no. 1, 1969.

[21] R. G. Brown and P. Y. C. Hwang, *Introduction to Random Signals and Applied Kalman Filtering*, 3rd ed. New York: Wiley, 1997.

[22] E. R. Bachmann and D. L. Gay, "Design and evaluation of an integrated GPS/INS system for shallow-water AUV navigation," Master's thesis, Naval Postgraduate School, Monterey, CA, Sept. 1995.

[23] *Model TRT-7 Tilting Rotary Table*, Hass Automation, Inc., Chatsworth, CA, July 1992.

[24] R. Wolf, G. W. Hein, B. Eissfeller, and E. Loehnert, "An integrated low cost GPS/INS attitude determination and position location system," in *Proc. ION GPS-96 Meeting*, Kansas City, MO, Sept. 1996, pp. 975–981.

[25] R. Knapp, "Calibration and evaluation of a water speed indicator and compass for the small autonomous underwater vehicle navigation filter," Master's thesis, Naval Postgraduate School, Monterey, CA, Dec. 1997.

[26] X. Yun, G. C. Hernandez, E. R. Bachmann, R. B. McGhee, and A.J. Healey, "An integrated GPS/INS navigation system for small AUV's using an asynchronous Kalman filter," in *Proc. IEEE Conf. Autonomous Underwater Vehicle (AUV'98)*, Cambridge, MA, Aug. 1998.